A Highly Sensitive Nanopore Platform for Measuring RNase A Activity

Haiyan Zheng[a], Sathishkumar Munusamy[a], Pearl Arora[b], Rana Jahani[a], and Xiyun Guan[a,]*

[a] Department of Chemistry, University of Missouri, Columbia, MO 65211, USA
[b] Department of Chemistry, Illinois Institute of Technology, Chicago, IL, 60616, USA

*Corresponding Author e-mail: xgpc2@missouri.edu

Abstract

Ribonuclease A (RNase A) plays significant roles in several physiological and pathological conditions and can be used as a valuable diagnostic biomarker for human diseases such as myocardial infarction and cancer. Hence, it is of great importance to develop a rapid and cost-effective method for the highly sensitive detection of RNase A. The significance of RNase A assay is further enhanced by the growing attention from the biotechnology and pharmaceutical industries to develop RNA-based vaccines and drugs in large part as a result of the successful development of mRNA vaccines in the COVID-19 pandemic. Herein, we report a label-free method for the detection of RNase A by monitoring its proteolytic cleavage of an RNA substrate in a nanopore. The method is ultra-sensitive with the limit of detection reaching as low as 30 femtogram per milliliter. Furthermore, sensor selectivity and the effects of temperature, incubation time, metal ion, salt concentration on sensor sensitivity were also investigated.

Key words: RNase A, biomarker, label-free analysis, enzyme assay, ultra-sensitive, nanopore

1. Introduction

The significant success of mRNA vaccines against COVID-19 has catalyzed a resurgence in the development of RNA-based vaccines and drugs for human diseases. One concern when performing experiments with RNA is contamination of ribonucleases (RNases) since RNA can readily be digested by them, thus having a profound effect on experimental data and/or downstream applications. To prevent/eliminate RNase contamination, regular RNase detection in the laboratory including lab benches, reagents, etc. is necessary. Among various RNases, RNase A is one of the hardiest enzymes in common laboratory usage due to its resistance to many harsh treatments such as autoclaving or prolonged boiling. Ribonuclease A is an important endonuclease which can not only cleave RNA at ribonucleotide uracil (rU) and cytosine (rC) residues, but also degrade rU / rC- containing chimeric DNA [1, 2]. Due to this feature, RNase A is often used for purifying DNA and/or protein samples by removing RNA contaminants [3]. Apart from RNA digestion, RNase A is also involved in a variety of physiological and pathological processes in organisms, such as cell proliferation, development, migration and invasion [4-6]. Therefore, it plays an important role in disease development and can be used as a valuable diagnostic biomarker for human diseases such as myocardial infarction and cancer [7-10]. In addition, RNase A has antiproliferative, cytotoxic, and antitumor activities, which offers the potential use as a candidate anti-cancer drug and is also an important target for drug discovery [11-13]. Thus, rapid and sensitive detection of RNase A is highly important. Traditional methods for RNase A activity detection includes gel electrophoresis [14], methylene blue [15], and radiolabeling assay [16]. These methods are time-consuming, have low sensitivity, and suffer from hazardous radiation and complicated operations. To overcome these issues, new detection techniques (e.g., electrochemical [17-20] and fluorescence-based [3, 21-23]) have been developed. However, most of these methods require the use of expensive fluorescently-labelled substrate and/or still involve with extensive procedure (e.g., immobilizing the substrate on the electrode).

Herein, we report an ultra-sensitive nanopore stochastic sensing method for detection of RNase A activity. During the past two decades, nanopore technology has attracted increasing interest and been utilized as a versatile tool to explore a wide variety of applications due to its advantages of rapid, label-free and single molecule analysis [24-31]. These include biosensing [32-39], DNA sequencing [40-44], pharmaceutical screening [45, 46], water desalination [47], medical diagnosis [48, 49], environmental monitoring [50] and so on. In this work, by monitoring the cleavage interaction between a RNA substrate and RNase A, highly sensitive (with a limit of detection down to 30 femtogram per milliliter) and selective detection of RNase A was successfully achieved. Our developed nanopore sensing strategy should have potential application in RNase contamination detection and disease diagnosis.

2. Experimental Section

2.1 Materials and Reagents

RNase A (from bovine pancreas), bovine serum albumin (BSA), Trizma base, sodium chloride (NaCl), glycerol, trypsin (from bovine pancreas), deoxyribonuclease (DNase, from bovine pancreas), and albumin from human serum (HSA) were purchased from Sigma-Aldrich (St. Louis, MO). A 22-mer microRNA (miRNA, sequence: 5’-rCrUrGrUrGrCrGrUrGrUrGrArCrArGrCrGrGrCrUrGrA-3’) was synthesized from Integrated DNA Technologies (Coralville, IA). Except for the electrolyte buffer solution used in single-channel recordings, which was prepared with HPLC-grade water (ChromAR, Mallinchkrodt Baker), all the other solutions were prepared with Nuclease-free water (Sigma-Aldrich, St. Louis, MO).

2.2 Electrical Recording and Data Analysis

The microRNA (miRNA) or miRNA/RNase A mixture sample was analyzed using a mutant $(M113K)_7$ α-hemolysin (α-HL) nanopore in a traditional 2-comartment bilayer setup using a procedure as described previously [24, 51]. Current modulations were recorded with an electrophysiology system consisting of Axopatch 200B amplifier and Digidata 1550B converter (Molecular Devices, Sunnyvale, CA). Data analysis was carried out by using clampfit software (Molecular Devices). It should be noted that the substrate miRNA used in this study contains many cleavage sites. After its digestion by RNase A, a variety of small miRNA fragments with different lengths might be produced, thus causing current modulations with complicated features in the nanopore. To simplify data analysis, the cleavage percentage of the substrate instead of the generated new fragment events was used to measure the activity of RNase A.

3. Results and Discussion

3.1 Detection Strategy and Measurement of RNase A Activity

The strategy for the detection of RNase A is shown in Scheme 1. Briefly, in the absence of RNase A, current modulations are caused only by the substrate. However, in the presence of RNase A, it will cleave the substrate and produce shorter RNA fragments, and thus producing events with different signatures (usually having smaller duration and blockage amplitude). Therefore, by comparing these events (in the absence and presence of RNase A), the activity of RNase A can be determined.

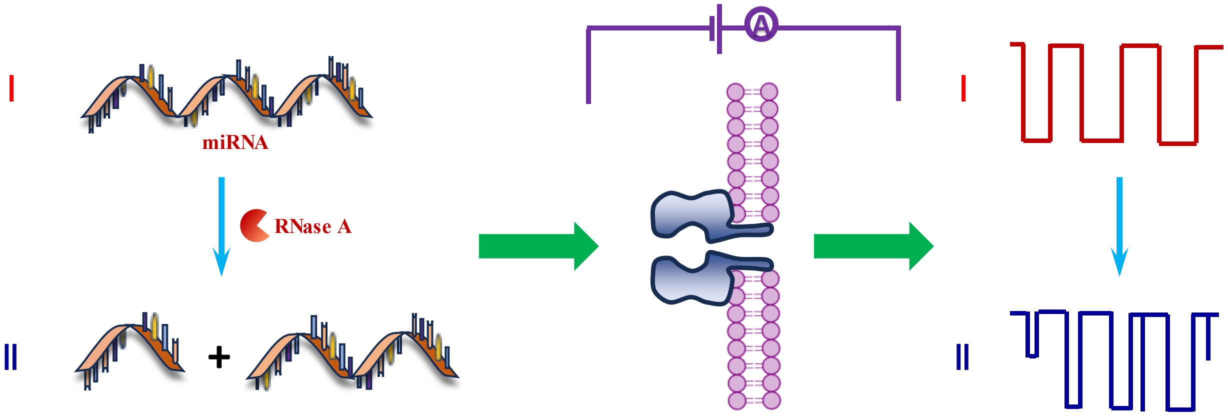

Scheme 1. Schematic representation of the strategy of nanopore detection of RNase A. (Ⅰ) Without the enzyme, the current modulations are caused only by the substrate. (Ⅱ) With the enzyme, in addition to a decrease in the frequency of the substrate events, new current modulations having residence time and/or amplitude values that differ from those of the substrate might be observed because of the cleavage fragments as a result of the enzymatic reaction.

To demonstrate this strategy, RNase A cleavage of miRNA was first investigated with an α-hemolysin (α-HL), $(M113K)_7$, nanopore at + 180 mV in 1 M NaCl and 10 mM Tris (pH 7.5) solution. The $(M113K)_7$ α-HL nanopore was produced by replacing the methionine residues at position 113 of the wild-type α-HL by lysine amino acids via site-directed mutagenesis, followed by coupled in vitro transcription and translation [52]. Compared with the wild type α-HL pore, this engineered nanopore provides a better resolution to the detection of charged species [51-53]. The applied potential bias of +180 mV was chosen based on our previous studies [54], at which the nucleic acid translocation event frequency is relatively large, without compromising the stability of the supporting lipid bilayer. Our experimental results were summarized in Fig. 1a. Clearly, without RNase A, the translocation of the miRNA molecule in the α-HL nanopore produced two major types of events (i.e., deep blockades and shallow blockades). The deep blockades had a narrow range of amplitudes (with ~ 99% channel block) and a large mean duration value (80.6 ± 2.0 ms) but with a broad distribution (~ 3 orders) of residence time, while the shallow blockades showed a small mean residence time (1.7 ± 0.1 ms) and a wide range of amplitudes (from ~ 93% to almost full channel block). These two types of events might be attributed to the different orientations in which miRNA entered and passed through the nanopore (5' to 3' entrance and 3' to 5' entrance). Note that this phenomenon has been reported previously [37, 55-57]. It is also likely that some small amplitude and small residence time events were due to the failure of translocation through the constriction after the miRNA molecule entered the vestibule of α-HL, but instead escaped immediately backward, or just collided with the *cis* opening of the pore [58, 59]. In contrast, in the presence of RNase A, we observed a significant decrease in the event frequency of the substrate miRNA. Furthermore, with an increase in the concentration of RNase A, the event frequency for both shallow blockades and deep blockades decreased, suggesting that the miRNA molecules are being cleaved by the RNase A (note that, the possibility that RNase A would block the nanopore, thus interfering with the study of its effect on miRNA transport was ruled out by the control experiment, where the presence of RNase A alone in the solution rarely produced current modulations in the nanopore (Fig. S1)). Since the substrate contains many RNase A cleavage sites, some of the fragments produced after digestion are a few bases or shorter in length, so that they would translocate through the nanopore too rapidly to be picked up by the nanopore sensor, as demonstrated in previous studies [58]. To simplify data analysis, only the events with the residence time more than 9.5 ms (with ~ 98% to full channel block) were included.

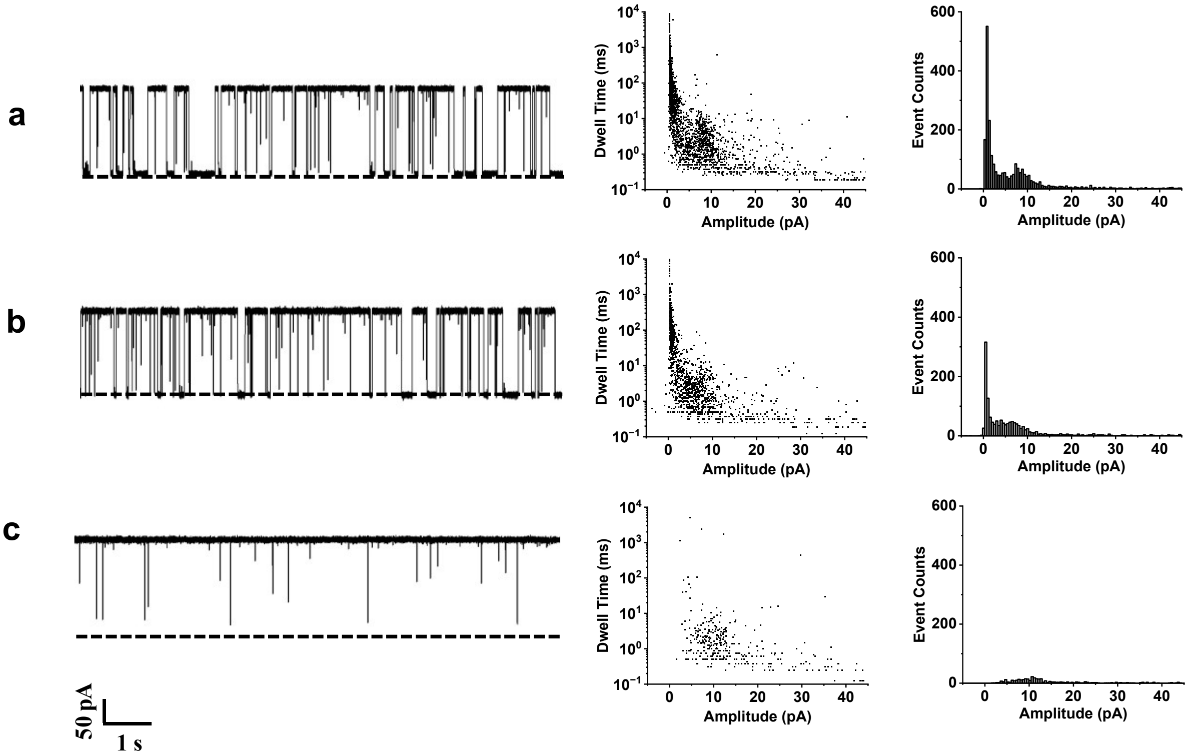

Fig. 1. Nanopore measurement of RNase A activity: (a) 0 ng/mL; (b) 0.5 ng/mL; and (c) 1 ng/mL. (*Left*) typical single-channel current recording trace segments. Dashed lines represent the level of zero current; (*middle*) the corresponding scatter plots of event amplitude versus residence time; and (*right*) event amplitude histograms. The experiments were performed at + 180 mV in symmetric electrolyte solutions containing 1 M NaCl and 10 mM Tris (pH 7.5) with the $(M117K)_7$ α-hemolysin pore. In Figs. 1b and 1c, the miRNA-RNase A mixtures were incubated in a 10.5 μL of solution containing 0.5 M NaCl, 2.5 mM Mg^{2+}, and 5 mM Tris (pH 7.5) at 37 °C for 30 minutes, followed by analysis with the nanopore platform without further RNase A deactivation. The concentration of miRNA used was 0.5 μM.

3.2 Effects of experimental conditions on the nanopore sensing sensitivity

It has been reported that the composition of the incubation buffer affects the enzyme activity [3]. In particular, for many enzymes (e.g., nucleases and proteases), they required metal ions as cofactors for functioning [25, 60]. Furthermore, salt concentration is another important factor that affects enzyme activity. To be more specific, depending upon its concentration, salt can deactivate or activate the enzyme. If the salt concentration is too high or too low, it would break the interactions in the tertiary structure of the enzyme, leading to a loss in its activity. To examine the effect of Mg^{2+} ions on nanopore detection of RNase A, the miRNA substrate (0.5 μM) and RNase A (0.5 ng/mL) mixtures were incubated at 37°C for 30 min in the absence and presence of Mg^{2+} ions, followed by nanopore analysis. Our experimental results showed that, compared with the incubation solution without Mg^{2+}, the presence of 2.5 mM Mg^{2+} led to 85 % increase in the substrate cleavage percentage (from 14.3 ± 2.2 % to 26.5 ± 1.1 %), confirming that Mg^{2+} ions indeed enhanced the RNase A activity and increased the nanopore sensor sensitivity (Fig. 2a). To investigate the salt effect on RNase digestion of miRNA, the mixture samples were incubated at 0.1 M NaCl and 0.5 M NaCl, respectively. The experimental results of nanopore analysis of these two samples were summarized in Fig. 2b. Clearly, the substrate cleavage percentage of the sample incubated at 0.1 M NaCl was almost three-fold larger than that at 0.5 M NaCl (97.4 ± 9.8 % vs. 26.4 ± 1.1 %).

Besides the buffer composition, incubation time and temperature also affect the catalytic activity of an enzyme. To determine the optimum incubation time, a series of experiments with miRNA digestion by RNase A with different incubation time was carried out. The results were summarized in Fig. 2c. Briefly, with an increase in the incubation time, the miRNA substrate cleavage percentage increased. For example, at a 10-min incubation time, 56.7 ± 2.0 % of the substrate was degraded, while 79.7 ± 13.5 % of miRNA was cleaved when the incubation time was increased to 45 min. For a rapid and sensitive RNase assay, 30 min (with 78.5 ± 11.7 % cleavage obtained) was selected as the optimum incubating time and used in the remaining experiments. In addition, the effect of the incubation temperature on the nanopore sensor resolution was also examined (Fig. 2d). The results showed that the substrate cleavage percentage increased by ~ 256 % (from 22.0 ± 6.0 % to 78.5 ± 11.7 %) as the incubation temperature increased from 22 °C to 37 °C. Thus, the incubation temperature of 37 °C was used in the remaining study.

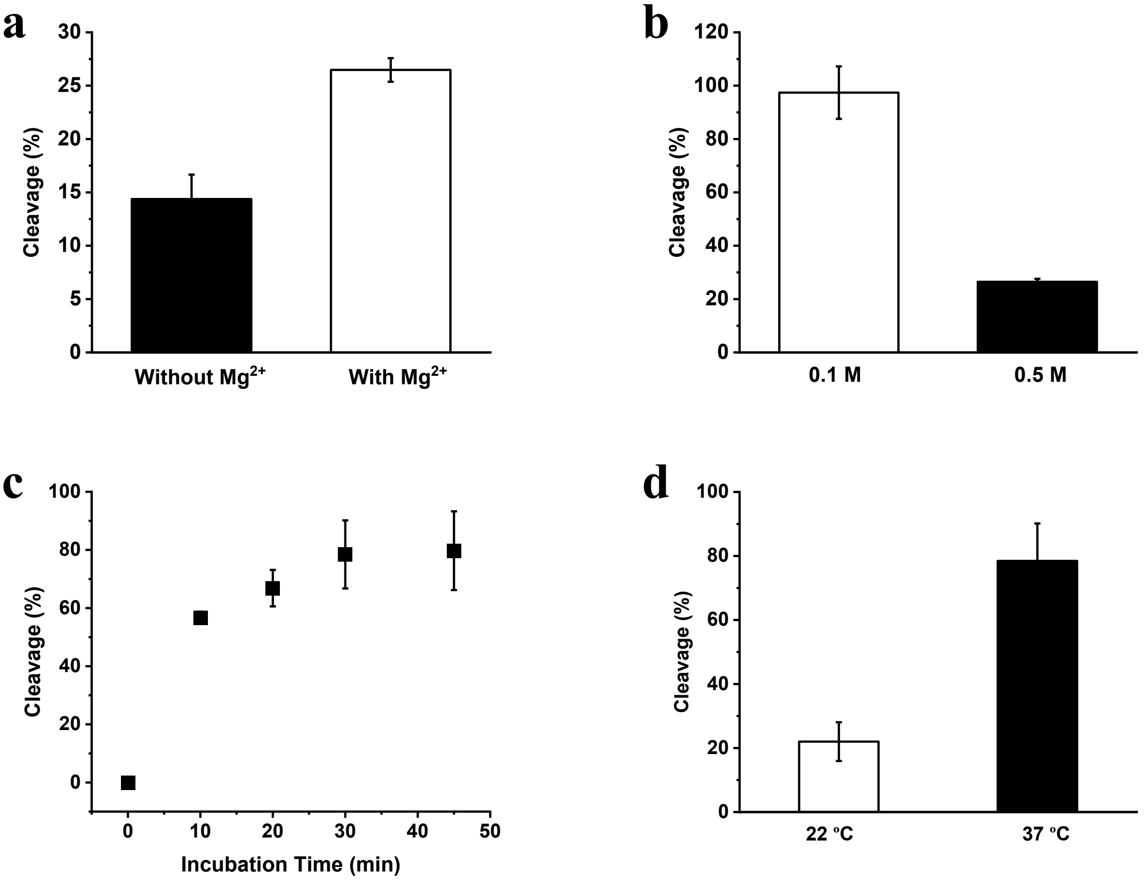

Fig. 2. Effects of (a) Mg^{2+} ions, (b) salt concentration, (c) incubation time and (d) temperature on the RNase A sensor sensitivity. The experiments were carried out in symmetric electrolyte solutions comprising 1 M NaCl and 10 mM Tris (pH 7.5) at + 180 mV. In Fig. 2a, the miRNA-RNase A mixtures were incubated in a 10.5 µL of solution containing 0.5 M NaCl and 5 mM Tris (pH 7.5) and in the absence or presence of 2.5 mM Mg^{2+} at 37°C for 30 minutes. In Fig. 2b, the mixtures were incubated in a solution containing 0.5 M NaCl, 2.5 mM Mg^{2+}, and 5 mM Tris (pH 7.5) as well as in a solution containing 0.1 M NaCl, 2.5 mM Mg^{2+}, and 5 mM Tris (pH 7.5), respectively. The concentration of RNase A used in Figs. 2a and b was 0.5 ng/mL. In Fig. 2c, the miRNA-RNase A mixtures were incubated in a 10.5 µL of solution containing 0.1 M NaCl, 2.5 mM Mg^{2+}, and 5 mM Tris (pH 7.5) at 37 °C for 0 to 45 minutes, while in Fig. 2d, the mixtures were incubated for 30 minutes at 22 °C and 37 °C, respectively. The concentration of RNase A used in Figs. 2c and d was 0.1 ng/mL. The concentration of the miRNA substrate used in Fig. 2 was 0.5 µM. The cleavage percentage of the substrate was obtained by using the equation: cleavage (%) = $(1 - f_s/f_0) \times 100\%$, where the value of f_s was the event frequency of miRNA after RNase A digestion, whereas the value of f_0 represented the event frequency of the substrate miRNA before enzyme cleavage.

3.3 Sensitivity and Selectivity of nanopore sensing

To investigate the sensitivity of our developed nanopore sensor, a series of experiments with digestion of miRNA by various concentrations of RNase A (ranging from 0.01 ng/mL to 0.5 ng/mL) was carried out where the concentration of miRNA was kept constant at 0.5 μM. We found that the miRNA substrate cleavage percentage increased with increasing RNase A concentration. The limit of detection (which is defined as the concentration of the target RNase A corresponding to the signal of the blank plus three times its standard deviation [61]) of the nanopore sensing was 4 pg/mL.

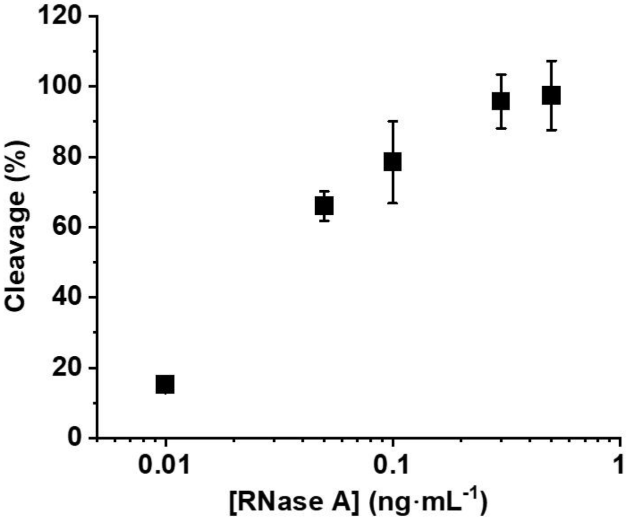

Fig. 3. Dose-response curve for RNase A detection. The experiments were carried out with the (M113K)$_7$ α-hemolysin pore in the buffer solutions containing 1 M NaCl and 10 mM Tris (pH 7.5) at + 180 mV. The miRNA-RNase A mixtures were incubated in a 10.5 μL of solution containing 0.1 M NaCl, 2.5 mM Mg^{2+}, and 5 mM Tris (pH 7.5) at 37 °C for 30 minutes before nanopore analysis. The concentration of miRNA was 0.5 μM.

To improve the sensor sensitivity, nanopore analysis of miRNA cleavage by RNase A was further investigated under asymmetric electrolyte conditions (i.e., salt gradients). Using a salt gradient instead of the symmetric electrolyte solution is a well-established strategy to enhance the performance of the nanopore sensor, especially in the analysis of charged analytes [62, 63]. As expected, we found that compared with the symmetric electrolyte solution of 1 M NaCl (*cis*) / 1 M NaCl (*trans*) (event frequency: ~ 8.2 s^{-1}•μM^{-1}), a more than 10-fold increase in the miRNA event frequency was obtained in the salt gradient of 1 M NaCl (*cis*) / 3 M NaCl (*trans*) (event frequency: ~ 86 s^{-1}•μM^{-1}). Apart from increasing the event frequency to improve the detection limit of the nanopore, we also attempted to increase the sensor signal-to-noise ratio by reducing the number of background events. We found that, under an asymmetric electrolyte condition of 3 M NaCl (*cis*) / 1 M NaCl (*trans*), the LOD (also defined as the concentration of the target RNase A corresponding to the signal of the blank plus three times its standard deviation) of the nanopore-based RNase A sensor could reach as low as 30 femtogram per milliliter (Fig. 4 and Supporting Information, Fig. S2) in spite of a decrease in the frequency of the substrate events (~ 7 s^{-1} •μM^{-1}). To our best knowledge, such a detection limit is ~ 1 to 3 orders better than those of other reported highly sensitive RNase A detection methods (e.g., electrochemiluminescence (0.2 pg/mL) [1], electrochemical (4 - 10 pg/mL) [17, 18], and fluorescence (98 pg/mL) [6]).

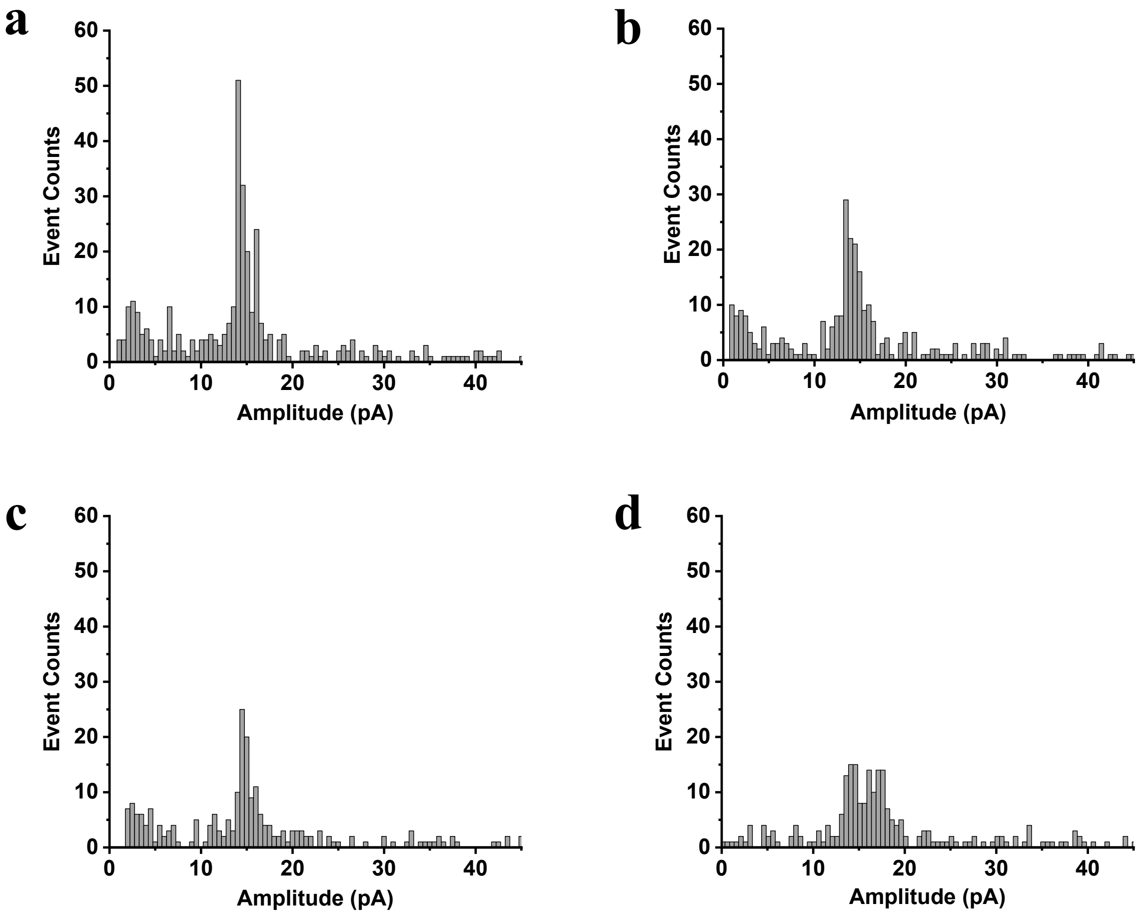

Fig. 4. Effect of salt gradient on RNase A detection. a) 0; b) 0.1; c) 1; and d) 3 pg/mL RNase A. The experiments were performed at +180 mV with the $(M113K)_7$ α-HL nanopore in a salt gradient of 3 M NaCl and 10 mM Tris (pH 7.5) (*cis*) / 1 M NaCl and 10 mM Tris (pH 7.5) (*trans*) and in the presence of 50 nM miRNA. The event counts were calculated based on 20-min single channel recording trace segments.

To investigate the selectivity of this nanopore sensing system, two enzymes (trypsin and DNase) and two proteins (HSA and BSA) were examined. Among them, HSA (short for human serum albumin) is the most abundant blood protein in humans and has many vital biological roles, while BSA is the most abundant plasma protein in bovines and is often used as a protein concentration standard in lab experiments. On the other hand, trypsin is the most important digestive enzyme produced in the pancreas, while DNases are enzymes that catalyze the hydrolytic cleavage of phosphodiester linkages in the DNA backbone, thus degrading DNA. Our experiments showed that these four species could be divided into two categories. Briefly, as shown in Fig. 5, in the presence of trypsin and DNase, the substrate events decreased by 9.6 ± 1.0 % and 10.6 ± 0.5 %, respectively. In contrast, the existence of HSA or BSA in the solution led to an increase (10.6 ± 0.2 % and 10.2 ± 0.3 %) in the substrate event count. Hence, their interfering effect is negligible since 95.8 % cleavage in the miRNA substrate was observed in the presence of RNase A.

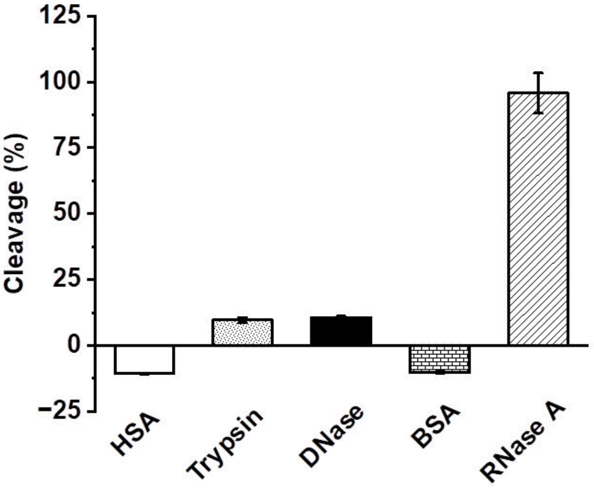

Fig. 5. Selectivity of the nanopore sensing system. The experiments were performed at +180 mV with the $(M113K)_7$ α-hemolysin pore in symmetric electrolyte buffer solutions containing 1 M NaCl and 10 mM Tris (pH 7.5). The miRNA-enzyme or protein mixture samples were incubated in a 10.5 µL of solution containing 0.1 M NaCl, 2.5 mM Mg^{2+}, and 5 mM Tris (pH 7.5) for 30 min at 37 °C. The concentration of miRNA was 0.5 µM, while those of enzymes/proteins were 0.1 ng/mL each.

4. Conclusion

In summary, by monitoring the enzymatic cleavage of a miRNA substrate using a nanopore, a label-free single-molecule sensing system was developed to measure the activity of RNase A. Our method is rapid, selective, and highly sensitive, with a limit of detection down to 30 femtogram per milliliter. It should be noted that this sensor was not optimized since the miRNA substrate used in this work contained multiple cleavage sites, so that a mixture of short RNA fragments with different length was produced after RNase cleavage, generating current modulation events with complicated features in the nanopore. To simplify data analysis, the activity of RNase reported in this study was determined based on the decrease in the frequency of the substrate events. It is likely that the sensitivity and LOD of the nanopore sensor might be further improved by using a substrate containing only a single cleavage site and analyzing the enzyme activity based on an increase in the event frequency of the degradation products. In fact, using such a strategy for nuclease assay is currently underway in our laboratory. Moreover, the performance of the sensor maybe further improved by using a larger salt gradient than that used in this work. Given the high sensitivity of the method, and the importance of RNase contamination detection as well as its role as valuable diagnostic/prognostic markers for human diseases and as important targets for drug discovery, our developed nanopore sensing strategy may find potential applications in real-world sample analysis.

Author contributions

Haiyan Zheng: Investigation, Methodology, Data curation, Formal analysis, Writing - original draft. **Sathishkumar Munusamy:** Investigation. **Pearl Arora:** Investigation. **Rana Jahani:** Investigation. **Xiyun Guan:** Conceptualization, Supervision, Project administration, Writing - review & editing.

Declaration of Competing Interest

The authors declare that they have no known competing financial interests or personal relationships that could have appeared to influence the work reported in this paper.

Acknowledgments

This work was financially supported by the National Institutes of Health (R01GM147247) and National Science Foundation (2203763 and 2345813).

References

[1] J. Ni, H. Lin, W. Yang, Y. Liao, Q. Wang, F. Luo, L. Guo, B. Qiu, Z. Lin, Homogeneous electrochemiluminescence biosensor for the detection of RNase A activity and its inhibitor, Anal. Chem. 91(22) (2019) 14751-14756.

[2] S. Sato, S. Takenaka, Highly sensitive nuclease assays based on chemically modified DNA or RNA, Sens. (2014) 12437-12450.

[3] C. Tong, C. Zhao, B. Liu, B. Li, Z. Ai, J. Fan, W. Wang, Sensitive detection of RNase A activity and collaborative drug screening based on rGO and fluorescence probe, Anal. Chem. 90(4) (2018) 2655-2661.

[4] S. Ibaragi, N. Yoshioka, S. Li, M.G. Hu, S. Hirukawa, P.M. Sadow, G.-f. Hu, Neamine inhibits prostate cancer growth by suppressing angiogenin-mediated rRNA transcription, Clin. Cancer Res. 15(6) (2009) 1981-1988.

[5] J. Sheng, W. Yu, X. Gao, Z. Xu, G.-F. Hu, Angiogenin stimulates ribosomal RNA transcription by epigenetic activation of the ribosomal DNA promoter, J. Cell. Phys. 229(4) (2014) 521-529.

[6] W. Dang, R. Luo, J. Fan, Y. Long, C. Tong, F. Xiao, X. Xiong, B. Liu, RNase A activity analysis and imaging using label-free DNA-templated silver nanoclusters, Talanta 209 (2020) 120512.

[7] W.-C. Kim, C.H. Lee, The role of mammalian ribonucleases (RNases) in cancer, Biochimica et Biophysica Acta – Rev. Cancer 1796(2) (2009) 99-113.

[8] L.I. Hernandez, M.J. Araúzo-Bravo, D. Gerovska, R.R. Solaun, I. Machado, A. Balian, J. Botero, T. Jiménez, O. Zuriarrain Bergara, L. Larburu Gurruchaga, A. Urruticoechea, F.J. Hernandez, Discovery and proof-of-concept study of nuclease activity as a novel biomarker for breast cancer tumors, Cancers (2021).

[9] Y. Peng, L. Li, M. Huang, C. Duan, L. Zhang, J. Chen, Angiogenin interacts with ribonuclease inhibitor regulating PI3K/AKT/mTOR signaling pathway in bladder cancer cells, Cell. Signal. 26(12) (2014) 2782-2792.

[10] D. Basso, C. Fabris, A. Meani, G. Del Favero, A. Panucci, D. Vianello, A. Piccoli, R. Naccarato, Serum deoxyribonuclease and ribonuclease in pancreatic cancer and chronic pancreatitis, Tumori J. 71(6) (1985) 529-532.

[11] X. Si, S. Ma, Y. Xu, D. Zhang, N. Shen, H. Yu, Y. Zhang, W. Song, Z. Tang, X. Chen, Hypoxia-sensitive supramolecular nanogels for the cytosolic delivery of ribonuclease A as a breast cancer therapeutic, J. Controlled Release 320 (2020) 83-95.

[12] I.S. Mohamed, A.V. Sen'kova, O.V. Markov, A.V. Markov, I.A. Savin, M.A. Zenkova, N.L. Mironova, bovine pancreatic RNase A: an insight into the mechanism of antitumor activity in vitro and in vivo, Pharm. 14 (2022) 1173.

[13] O.A. Shklyaeva, N.L. Mironova, E.M. Malkova, O.S. Taranov, E.I. Ryabchikova, M.A. Zenkova, V.V. Vlasov, Cancer-suppressive effect of RNase A and DNase I, Dokl. Biochem. Biophys. 420(1) (2008) 108-111.

[14] A. Blank, R.H. Sugiyama, C.A. Dekker, Activity staining of nucleolytic enzymes after sodium dodecyl sulfate-polyacrylamide gel electrophoresis: Use of aqueous isopropanol to remove detergent from gels, Anal. Biochem. 120(2) (1982) 267-275.

[15] T. Greiner-Stoeffele, M. Grunow, U. Hahn, A general ribonuclease assay using methylene blue, Anal. Biochem. 240(1) (1996) 24-28.

[16] J.S. Roth, S.W. Milstein, Ribonuclease: I. a new assay method with P32-labled yeast ribonucleic acid. J. Biol. Chem. 196(2) (1952) 489-498.

[17] S. Sato, S. Takenaka, Electrochemical RNase A detection using an electrode with immobilized ferrocenyl deoxyribooligonucleotide containing cytidine residue, Electroanalysis 25(7) (2013) 1652-1658.

[18] Y. Ye, W. Wen, Y. Xiang, X. Qi, J.T. La Belle, J.J.L. Chen, J. Wang, Direct electrochemical monitoring of RNase activity, Electroanalysis 20(8) (2008) 919-922.

[19] M. Kanazawa, S. Sato, K. Ohtsuka, S. Takenaka, Electrochemical RNase detection using ferrocenylnaphthalene diimide, Nucleic Acids Symp. Ser. 51(1) (2007) 323-324.

[20] Y. Ying, M. Zhou, S. Dai, M. Ma, W. Deng, Y. Tan, Q. Xie, Au nanoparticles/SnO_2/$ZnIn_2S_4$-based biosensor for photoelectrochemical/electrochemical dual-signal detection of RNase A by combining the enzymolysis of DNA probe and the generation of molybdophosphate precipitate, Sens. Actuators B: Chem. 354 (2022) 131251.

[21] J.-W. Choi, B.M.K. Vasamsetti, K.-W. Kim, S.H. Seo, D.-H. Lee, S.-I. Chang, J. Choo, H.Y. Kim, Analysis of ribonuclease activity in sub-nanoliter droplets by label-free fluorescence measurements, Analyst 142(14) (2017) 2610-2616.

[22] C. Tong, Y. Hu, Q. Xie, T. Zhou, J. Fan, Y. Qin, B. Liu, W. Wang, Sensitive RNase A detection and intracellular imaging using a natural compound-assisted tetrahedral DNA nanoprobe, Chem. Commun. 56(21) (2020) 3229-3232.

[23] J. Du, H. Yang, N. Huang, Y. Dong, Q. Gao, W. Yang, B. Liu, C. Yang, Highly sensitive and selective RNase A recognition systems based on “OFF – ON – OFF” fluorescence probes, Sens. Actuators B: Chem. 259 (2018) 282-288.

[24] Q. Zhao, R.S.S. de Zoysa, D. Wang, D.A. Jayawardhana, X. Guan, Real-time monitoring of peptide cleavage using a nanopore probe, J. Am. Chem. Soc. 131(18) (2009) 6324-6325.

[25] S. Zhou, L. Wang, X. Chen, X. Guan, Label-free nanopore single-molecule measurement of trypsin activity, ACS Sens. 1(5) (2016) 607-613.

[26] S. Majd, E.C. Yusko, Y.N. Billeh, M.X. Macrae, J. Yang, M. Mayer, Applications of biological pores in nanomedicine, sensing, and nanoelectronics, Curr. Opin. Biotechnol. 21(4) (2010) 439-476.

[27] C. Shasha, R.Y. Henley, D.H. Stoloff, K.D. Rynearson, T. Hermann, M. Wanunu, Nanopore-based conformational analysis of a viral RNA drug target, ACS Nano 8(6) (2014) 6425-6430.

[28] Y. Zhang, X. Chen, C. Wang, H.-C. Chang, X. Guan, Nanoparticle-assisted detection of nucleic acids in a polymeric nanopore with a large pore size, Biosens. Bioelectron. 196 (2022) 113697.

[29] Q. Palomar, A. Svärd, S. Zeng, Q. Hu, F. Liu, D. Aili, Z. Zhang, Detection of gingipain activity using solid state nanopore sensors, Sens. Actuators B: Chem. 368 (2022) 132209.

[30] Y. Zhang, X. Chen, C. Wang, G.M. Roozbahani, H.-C. Chang, X. Guan, Chemically functionalized conical PET nanopore for protein detection at the single-molecule level, Biosens. Bioelectron. 165 (2020) 112289.

[31] Z. Su, Y. Kong, T. Li, Y. Zhao, X. Zhang, D. Wu, Y. Wu, G. Li, An aptamer-triggered hybridization chain reaction strategy for ultra-sensitive biological nanopore detection of aflatoxin B1, Sens. Actuators B: Chem. 407 (2024) 135457.

[32] G.M. Roozbahani, X. Chen, Y. Zhang, L. Wang, X. Guan, Nanopore detection of metal Ions: current status and future directions, Small Methods 4(10) (2020) 2000266.

[33] L. Wang, X. Chen, S. Zhou, G.M. Roozbahani, Y. Zhang, D. Wang, X. Guan, Displacement chemistry-based nanopore analysis of nucleic acids in complicated matrices, Chem. Commun. 54(99) (2018) 13977-13980.

[34] L. Mereuta, A. Asandei, I. Schiopu, Y. Park, T. Luchian, Nanopore-assisted, sequence-specific detection, and single-molecule hybridization analysis of short, single-stranded DNAs, Anal. Chem. 91(13) (2019) 8630-8637.

[35] J. Shim, S. Banerjee, H. Qiu, K.K.H. Smithe, D. Estrada, J. Bello, E. Pop, K. Schulten, R. Bashir, Detection of methylation on dsDNA using nanopores in a MoS_2 membrane, Nanoscale 9(39) (2017) 14836-14845.

[36] H.-Y. Wang, Z. Gu, C. Cao, J. Wang, Y.-T. Long, Analysis of a single α-synuclein fibrillation by the interaction with a protein nanopore, Anal. Chem. 85(17) (2013) 8254-8261.

[37] X. Chen, G. M. Roozbahani, Z. Ye, Y. Zhang, R. Ma, J. Xiang, X. Guan, Label-free detection of DNA mutations by nanopore analysis, ACS Appl. Mater. Interfaces 10(14) (2018) 11519-11528.

[38] A. Apetrei, A. Ciuca, J.-k. Lee, C.H. Seo, Y. Park, T. Luchian, A protein nanopore-based approach for bacteria sensing, Nanoscale Res. Lett. 11(1) (2016) 501.

[39] D.M.M. Krishantha, Z.S. Breitbach, N.L.T. Padivitage, D.W. Armstrong, X. Guan, Rapid determination of sample purity and composition by nanopore stochastic sensing, Nanoscale 3(11) (2011) 4593-4596.

[40] Y. Wang, Y. Zhao, A. Bollas, Y. Wang, K.F. Au, Nanopore sequencing technology, bioinformatics and applications, Nat. Biotechnol. 39(11) (2021) 1348-1365.

[41] Y.-L. Ying, Z.-L. Hu, S. Zhang, Y. Qing, A. Fragasso, G. Maglia, A. Meller, H. Bayley, C. Dekker, Y.-T. Long, Nanopore-based technologies beyond DNA sequencing, Nat. Nanotechnol. 17(11) (2022) 1136-1146.

[42] C. Koch, B. Reilly-O'Donnell, R. Gutierrez, C. Lucarelli, F.S. Ng, J. Gorelik, A.P. Ivanov, J.B. Edel, Nanopore sequencing of DNA-barcoded probes for highly multiplexed detection of microRNA, proteins and small biomarkers, Nat. Nanotechnol. 18(12) (2023) 1483-1491.

[43] M.T. Hwang, M. Heiranian, Y. Kim, S. You, J. Leem, A. Taqieddin, V. Faramarzi, Y. Jing, I. Park, A.M. van der Zande, S. Nam, N.R. Aluru, R. Bashir, Ultrasensitive detection of nucleic acids using deformed graphene channel field effect biosensors, Nat. Commun. 11(1) (2020) 1543.

[44] Z.-L. Hu, M.-Z. Huo, Y.-L. Ying, Y.-T. Long, Biological nanopore approach for single-molecule protein sequencing, Angew. Chem. Int. Ed. 60(27) (2021) 14738-14749.

[45] M.B. Steffensen, D. Rotem, H. Bayley, Single-molecule analysis of chirality in a multicomponent reaction network, Nature Chemistry 6(7) (2014) 603-607.

[46] X.-f. Kang, S. Cheley, X. Guan, H. Bayley, Stochastic detection of enantiomers, J. Am. Chem. Soc. 128(33) (2006) 10684-10685.

[47] M. Heiranian, A.B. Farimani, N.R. Aluru, Water desalination with a single-layer MoS_2 nanopore, Nat. Commun. 6(1) (2015) 8616.

[48] S. Wang, F. Haque, P.G. Rychahou, B.M. Evers, P. Guo, Engineered nanopore of Phi29 DNA-packaging motor for real-time detection of single colon cancer specific antibody in serum, ACS Nano 7(11) (2013) 9814-9822.

[49] Y. Wang, D. Zheng, Q. Tan, M.X. Wang, L.-Q. Gu, Nanopore-based detection of circulating microRNAs in lung cancer patients, Nat. Nanotechnol. 6(10) (2011) 668-674.

[50] T. Li, Z. Su, Y. Li, L. Xi, G. Li, An aptamer-assisted biological nanopore biosensor for ultra-sensitive detection of ochratoxin A with a portable single-molecule measuring instrument, Talanta 248 (2022) 123619.

[51] Y. Han, S. Zhou, L. Wang, X. Guan, Nanopore back titration analysis of dipicolinic acid, Electrophor. 36(3) (2015) 467-470.

[52] Q. Zhao, D. Wang, D.A. Jayawardhana, X. Guan, Stochastic sensing of biomolecules in a nanopore sensor array, Nanotechnology 19(50) (2008) 505504.

[53] M. Montal, P. Mueller, Formation of bimolecular membranes from lipid monolayers and a study of their electrical properties, Proc. Natl. Acad. Sci. 69(12) (1972) 3561-3566.

[54] A. Liu, Q. Zhao, D.M.M. Krishantha, X. Guan, Unzipping of double-stranded DNA in engineered α-hemolysin pores, J. Phys. Chem. Lett. 2(12) (2011) 1372-1376.

[55] J. Muzard, M. Martinho, J. Mathé, U. Bockelmann, V. Viasnoff, DNA translocation and unzipping through a nanopore: some geometrical effects, Biophys. J. 98(10) (2010) 2170-2178.

[56] J. Mathé, A. Aksimentiev, D.R. Nelson, K. Schulten, A. Meller, Orientation discrimination of single-stranded DNA inside the α-hemolysin membrane channel, Proc. Natl. Acad. Sci. 102(35) (2005) 12377-12382.

[57] L. Wang, Y. Han, S. Zhou, G. Wang, X. Guan, Nanopore biosensor for label-free and real-time detection of anthrax lethal factor, ACS Appl. Mater. Interfaces 6(10) (2014) 7334-7339.

[58] R.S.S. de Zoysa, D.M.M. Krishantha, Q. Zhao, J. Gupta, X. Guan, Translocation of single-stranded DNA through the α-hemolysin protein nanopore in acidic solutions, Electrophor. 32(21) (2011) 3034-3041.

[59] T.Z. Butler, J.H. Gundlach, M. Troll, Ionic current blockades from DNA and RNA molecules in the α-hemolysin nanopore, Biophys. J. 93(9) (2007) 3229-3240.

[60] Y. Zhang, X. Chen, G.M. Roozbahani, X. Guan, Rapid and sensitive detection of the activity of ADAM17 using a graphene oxide-based fluorescence sensor, Analyst 144(5) (2019) 1825-1830.

[61] H.-M. Chan, H.-W. Li, Multifunctional encoded self-assembling protein nanofibrils as platform for high-throughput and multiplexed detection of biomolecules, Anal. Chem. 83(24) (2011) 9370-9377.

[62] M. Wanunu, W. Morrison, Y. Rabin, A.Y. Grosberg, A. Meller, Electrostatic focusing of unlabelled DNA into nanoscale pores using a salt gradient, Nat. Nanotechnol. 5(2) (2010) 160-165.

[63] G.M. Roozbahani, X. Chen, Y. Zhang, R. Xie, R. Ma, D. Li, H. Li, X. Guan, Peptide-mediated nanopore detection of uranyl ions in aqueous media, ACS Sens. 2(5) (2017) 703-709.